Smart Structures and Systems, *Vol. 15, No. 1 (2015) 57-80*
DOI: http://dx.doi.org/10.12989/sss.2015.15.1.057

A two-stage and two-step algorithm for the identification of structural damage and unknown excitations: numerical and experimental studies

Ying Lei*, Feng Chen and Huan Zhou

School of Architecture and Civil Engineering, Xiamen University, Xiamen 361005, China

(Received November 20, 2013, Revised March 10, 2014, Accepted April 5, 2014)

Abstract. Extended Kalman Filter (EKF) has been widely used for structural identification and damage detection. However, conventional EKF approaches require that external excitations are measured. Also, in the conventional EKF, unknown structural parameters are included as an augmented vector in forming the extended state vector. Hence the sizes of extended state vector and state equation are quite large, which suffers from not only large computational effort but also convergence problem for the identification of a large number of unknown parameters. Moreover, such approaches are not suitable for intelligent structural damage detection due to the limited computational power and storage capacities of smart sensors. In this paper, a two-stage and two-step algorithm is proposed for the identification of structural damage as well as unknown external excitations. In stage-one, structural state vector and unknown structural parameters are recursively estimated in a two-step Kalman estimator approach. Then, the unknown external excitations are estimated sequentially by least-squares estimation in stage-two. Therefore, the number of unknown variables to be estimated in each step is reduced and the identification of structural system and unknown excitation are conducted sequentially, which simplify the identification problem and reduces computational efforts significantly. Both numerical simulation examples and lab experimental tests are used to validate the proposed algorithm for the identification of structural damage as well as unknown excitations for structural health monitoring.

Keywords: Extended Kalman filter; two-stage; two-step; system identification; structural damage detection; unknown excitation; least- squares estimation

1. Introduction

In the past decades, numerous structural damage detection techniques have been proposed (Sohn *et al.* 2003, Wu *et al.* 2003, Feng 2009, Ou and Li 2010, Fan and Qiao 2011). Among them, techniques based on structural identification (SI) are useful as it is straightforward to identify structural damage by tracking the changes in the identified structural dynamic parameters (Ren *et al.* 2011, Li *et al.* 2011, Kim and Lynch 2012, Sirca and Adeli 2012). However, as an inverse problem, structural damage detection by conventional SI approaches is still a challenging task, e.g., it is desired to explore efficient algorithms for structural damage detection with partial

*Corresponding author, Professor, E-mail: ylei@xmu.edu.cn

http://www.techno-press.org/?journal=sss&subpage=8 ISSN: 1738-1584 (Print), 1738-1991 (Online)

measurements of structural responses(Yi *et al.* 2011, Lei *et al.* 2013, Kim *et al.* 2013).

On the other hand, intelligent structural damage detection based on smart sensor technology has received great attention in the last decade (Spencer *et al.* 2004, Lynch 2007, Yun and Min 2010). The intelligence of a smart sensor comes from the on-board microprocessor embedded with algorithms for self-signal processing, self-identification and self-diagnostics (Spencer *et al.* 2004, Sim *et al.* 2010, Yun *et al.* 2011) Therefore, it is necessary to investigate efficient algorithms for structural identification and damage detection which requires less computational effort and storage (Yun *et al.* 2011, Hsu *et al.* 2011, Park *et al.* 2013).

Extended Kalman filter (EKF) has shown its feasibility in structural identification with partial measurements of structural responses (Hoshiya and Sutoh 1993, Yang *et al*. 2006, Lei *et al.* 2012, Xu *et al.* 2012, Yuen *et al.* 2013). However, conventional EKF based approaches require that all excitation inputs are measured, which limits their utilizations in practice as it may be difficult or even impossible to measure all structural external excitations under actual operating conditions. In structural health monitoring (SHM), the knowledge of external excitation is important. Therefore, it is necessary to investigate algorithms for the identification of structures as well as the unknown external excitations. Yang *et al.* (2007) proposed an extended Kalman filter with unknown excitation inputs (EKF-UI), Lu and Law (2007) presented a method based on sensitivity of structural responses for identifying both the structural parameters and the excitations of a structure, Zhang *et al.* (2012) presented a method for simultaneous identification of excitations and structural damages, and Xu *et al.* (2012) studied structural parameters and dynamic loading identification form incomplete measurements. In these approaches, structural parameters and unknown excitations are identified simultaneously, which are quite cumbersome with much computation effort for accurate identification results.

Moreover, the extended state vector of a conventional EKF contains both the structural state vector of displacement and velocity responses and the unknown structural parametric vector, which results in large sizes of the extended state vector and the corresponding state equation (Hoshiya and Sutoh 1993). Since the state equation and the observation equation are highly non-linear with respect to the extended state vector, care should be taken for an EKF approach. Some approaches for the identification of structural state vector and unknown parameters in two-step have been presented to guarantee the stability and convergence of the numerical solution (Yang *et al.* 2006, 2007*)*. Also, substructure approaches have been proposed to improve the convergence of the structural parameters and reduce the computation effort (Koh *et al.* 1991). It has been shown that for an extended state vector with the order of 2n+m (n: number of structural DOFs, m: number of unknown structural parameters), the computational effort of the EKF is on the order of $(2n+m)^3$ (Liu *et al.* 2009). Therefore, conventional EKF approaches requirement of large computation effort and storage, which are not suitable for intelligent structural identification and damage detection due to the limited computational power and storage capacities of the micro-processor in a smart sensor. So far, some researchers have investigated algorithms to improve the performances of conventional EKF approaches (Wu *et al.* 2002, Lee and Yun 2008, Liu *et al.* 2009), especially Yang *et al.* (2006) and Huang *et al.* (2010) proposed the quadratic sum-squares error with unknown inputs (QSSE-UI) to identify structural parameters as well as unknown excitations in a two-step approach to reduce the computational efforts. Also, some researchers presented approaches of using derivative-free filtering procedures, like the unscented or particle ones (Julier *et al.* 2000, Wan and Van der Merwe 2001, Mariani and Ghisi 2007, Azam and Mariani 2012).

In this paper, a two-stage and two-step approach is proposed to remove the drawbacks of conventional EKF algorithms for the identification of structural damage as well as the unknown external excitations of a structure. In stage-one, structural state vector and unknown structural parameters are recursively estimated separately in a two-step Kalman estimator approach. In the first step, state vector is considered as an implicit function of the structural parameters (Huang *et al.* 2010, Yi *et al.* 2013), and the parametric vector is estimated directly by the Kalman estimator. In the second step, state vector of the structure is updated by the Kalman estimator. After the updated information of state vector and structural parameters, the unknown excitations are recursively estimated by least-squares estimation in stage-two. To test the effectiveness of the proposed algorithm, several numerical simulation examples and lab experimental tests are used.

The paper is organized as follows: Section 2 presents the proposed algorithm of two-stage and two-step Kalman estimator, Section 3 demonstrates the proposed algorithm by the numerical examples of the identification of structural damage and unknown excitations of the Phase-I IASC-ASCE benchmark building for SHM, a high-rise shear building, and a large size plan truss. Section 4 shows the experimental validations of the proposed approach by structural damage detection of a multi-story shear frame with joint damage under unknown ground excitation, a lab multi-story shear frame under unknown excitation, and a demonstration of intelligent structural damage detection using a smart sensor network embedded with the proposed algorithm.

2. The proposed two-stage and two-step algorithm

The equation of motion of a structure under some unknown external excitations can be written as

$$\boldsymbol{M}\ddot{\boldsymbol{x}} + \boldsymbol{F}\left[\boldsymbol{x}, \dot{\boldsymbol{x}}, \boldsymbol{\theta}\right] = \boldsymbol{G}\boldsymbol{f} + \boldsymbol{G}^u \boldsymbol{f}^u \tag{1}$$

where $\ddot{\boldsymbol{x}}$, $\dot{\boldsymbol{x}}$ and $\boldsymbol{x}$ are the vectors of structural acceleration, velocity, and displacement responses, respectively; $\boldsymbol{\theta}$ is the vector of unknown structural parameters; $\boldsymbol{F}\left[\boldsymbol{x}, \dot{\boldsymbol{x}}, \boldsymbol{\theta}\right]$ is the vector of internal force; $\boldsymbol{f}$ and $\boldsymbol{f}^u$ are the vectors of known and unknown external excitations, respectively; $\boldsymbol{G}$ and $\boldsymbol{G}^u$ are the influence matrices associated with $\boldsymbol{f}$ and $\boldsymbol{f}^u$, respectively. In general, the mass of the structure can be estimated accurately, so $\boldsymbol{M}$ is assumed known in this paper.

Eq. (1) can be rewritten in state equation as

$$\dot{\boldsymbol{X}} = \begin{Bmatrix} \dot{\boldsymbol{x}} \\ \boldsymbol{M}^{-1}\left(-\boldsymbol{F}\left[\boldsymbol{x}, \dot{\boldsymbol{x}}, \boldsymbol{\theta}\right] + \boldsymbol{G}\boldsymbol{f} + \boldsymbol{G}^u \boldsymbol{f}^u\right) \end{Bmatrix} = \boldsymbol{g}\left[\boldsymbol{X}, \boldsymbol{\theta}, \boldsymbol{f}, \boldsymbol{f}^u\right] \tag{2}$$

where $\boldsymbol{X} = [\boldsymbol{x}^{\mathrm{T}} \;\; \dot{\boldsymbol{x}}^{\mathrm{T}}]^T$ is the state vector of the structure.

It is assumed that a limited number of accelerometers are deployed in the structure to measure its acceleration responses. Therefore, the discretized observation equation can be expressed as

$$\boldsymbol{y}_k = \boldsymbol{D}\ddot{\boldsymbol{x}}_k + \boldsymbol{v}_k = -\boldsymbol{D}\boldsymbol{M}^{-1}\boldsymbol{F}\left[\boldsymbol{x}_k, \dot{\boldsymbol{x}}_k, \boldsymbol{\theta}\right] + \boldsymbol{B}\boldsymbol{f}_k + \boldsymbol{B}^u \boldsymbol{f}_k^{\mathrm{u}} + \boldsymbol{v}_k = \boldsymbol{h}\left(\boldsymbol{X}_k, \boldsymbol{\theta}_k, \boldsymbol{f}_k\right) + \boldsymbol{B}^u \boldsymbol{f}_k^{\mathrm{u}} + \boldsymbol{v}_k \tag{3}$$

in which, $\boldsymbol{y}_k$ is the measured acceleration at time $t = \mathrm{k} \times \Delta t$ with Δt being the sampling time step, $\boldsymbol{D}$ is the matrix denotes the locations of accelerometers deployed on the structure to measure its partial acceleration responses, $\boldsymbol{B} = \boldsymbol{D}\boldsymbol{M}^{-1}\boldsymbol{G}$, $\boldsymbol{B}^u = \boldsymbol{D}\boldsymbol{M}^{-1}\boldsymbol{G}^u$, and $\boldsymbol{v}_k$ is the measurement noise vector assumed to be a Gaussian white noise vector with zero mean and a covariance matrix $\boldsymbol{E}\left[\boldsymbol{v}_i\boldsymbol{v}_j^T\right] = \boldsymbol{R}_i\delta_{ij}$, where δ_{ij} is the Kroneker delta.

Instead of identifying structural state vector and unknown parameters simultaneously by forming an extended state vector in a EKF approach, a two-stage and two-step Kalman Estimator approach is proposed in this paper to remove the drawbacks of previous algorithms based on EKF.

2.1 Stage-one: Identification of structural system

In stage-one, structural state vector and unknown structural parameters are recursively estimated in a two-step Kalman estimator approach.

2.1.1. Step-one: estimation of the structural parameters

From Eq. (2), state vector $\boldsymbol{X}$ is an implicit function of the structural parameters $\boldsymbol{\theta}$ denoted by $\boldsymbol{X}(\boldsymbol{\theta})$. Differentiating both sides of Eq. (2) with respect to $\boldsymbol{\theta}$, one can derive the following equation as

$$\dot{\boldsymbol{X}}_{\boldsymbol{\theta}} = \frac{\partial \boldsymbol{g}(\boldsymbol{X}, \boldsymbol{\theta}, \boldsymbol{f}, \boldsymbol{f}^{\mathrm{u}})}{\partial \boldsymbol{\theta}} = \bar{\boldsymbol{g}}(\boldsymbol{X}_{\boldsymbol{\theta}}, \boldsymbol{X}(\boldsymbol{\theta}), \boldsymbol{\theta}) \tag{4}$$

where $\boldsymbol{X}_{\boldsymbol{\theta}}$ denotes $\dfrac{\partial \boldsymbol{X}}{\partial \boldsymbol{\theta}}$

Then, the recursive estimation of $\boldsymbol{X}_{\boldsymbol{\theta}}$ can be derived as

$$\boldsymbol{X}_{\boldsymbol{\theta},k+1|k} = \boldsymbol{X}_{\boldsymbol{\theta},k|k\text{-}1} + \int_{k\Delta t}^{(k+1)\Delta t} \bar{\boldsymbol{g}}(\boldsymbol{X}_{\boldsymbol{\theta},t|k}, \boldsymbol{X}(\boldsymbol{\theta}), \boldsymbol{\theta})dt \tag{5}$$

In step-one, recursive estimation of the structural parameters is derived based on Kalman estimator while state vector $\boldsymbol{X}$ is considered as an implicit function of the structural parameters $\boldsymbol{\theta}$. Then, Eq. (3) can be expressed as follows

$$\boldsymbol{y}_k = \boldsymbol{h}\left(\boldsymbol{X}(\boldsymbol{\theta}_k), \boldsymbol{\theta}_k, \boldsymbol{f}_k\right) + \boldsymbol{B}^{\mathrm{u}} \boldsymbol{f}_k^{\mathrm{u}} + \boldsymbol{v}_k \tag{6}$$

Let $\hat{\boldsymbol{\theta}}_k$ and $\hat{\boldsymbol{X}}_{k|k\text{-}1}$ denote the estimated $\boldsymbol{\theta}_k$ and $\boldsymbol{X}(\hat{\boldsymbol{\theta}}_k)$, respectively. $\boldsymbol{h}\left(\boldsymbol{X}_k(\boldsymbol{\theta}_k), \boldsymbol{\theta}_k, \boldsymbol{f}_k\right)$ is a nonlinear function of unknown vector $\boldsymbol{\theta}_k$ and can be linearized around $\hat{\boldsymbol{\theta}}_k$ through Taylor expand, i.e.

$$\boldsymbol{y}_{\mathrm{k}} = \boldsymbol{h}\left(\boldsymbol{X}(\boldsymbol{\theta}_{\mathrm{k}}), \boldsymbol{\theta}_{\mathrm{k}}, \boldsymbol{f}_{\mathrm{k}}\right) + \boldsymbol{B}^{\mathrm{u}} \boldsymbol{f}_k^{\mathrm{u}} + \boldsymbol{v}_{\mathrm{k}} = \boldsymbol{h}\left(\hat{\boldsymbol{X}}_{k|k-1}, \hat{\boldsymbol{\theta}}_k, \boldsymbol{f}_k\right) + \boldsymbol{H}_k\left(\boldsymbol{\theta}_k - \hat{\boldsymbol{\theta}}_k\right) + \boldsymbol{B}^{\mathrm{u}} \boldsymbol{f}_k^{\mathrm{u}} + \boldsymbol{v}_{\mathrm{k}} \tag{7}$$

in which, $\boldsymbol{H}_k$ can be derived by the chain rule of partial differentiation with respect to $\boldsymbol{\theta}_k$ as

$$\boldsymbol{H}_k = \boldsymbol{H}_{\boldsymbol{\theta},k} + \boldsymbol{H}_{X,k}\boldsymbol{X}_{\boldsymbol{\theta},k} \tag{8}$$

where

$$\boldsymbol{H}_{\theta,k} = \left[\frac{\partial \boldsymbol{h}(\boldsymbol{X},\boldsymbol{\theta},\boldsymbol{f})}{\partial \boldsymbol{\theta}}\right]_{X=\hat{X}_{k|k-1},\theta=\hat{\theta}_k} ;\ \boldsymbol{H}_{X,k} = \left[\frac{\partial \boldsymbol{h}(\boldsymbol{X},\boldsymbol{\theta},\boldsymbol{f})}{\partial \boldsymbol{X}}\right]_{X=\hat{X}_{k|k-1},\theta=\hat{\theta}_k} ;\ \boldsymbol{X}_{\theta,k} = \left[\frac{\partial \boldsymbol{X}}{\partial \boldsymbol{\theta}}\right]_{\theta=\hat{\theta}_k} \tag{9}$$

The structural parameters are time-invariant and can be estimated by the Kalman estimator as

$$\hat{\boldsymbol{\theta}}_{k+1} = \hat{\boldsymbol{\theta}}_k + \boldsymbol{K}_{\theta,k}\left[\boldsymbol{y}_k - \boldsymbol{h}\left(\hat{\boldsymbol{X}}_{k|k-1},\hat{\boldsymbol{\theta}}_k,\boldsymbol{f}_k\right) - \boldsymbol{B}^{\mathrm{u}}\hat{\boldsymbol{f}}^{\mathrm{u}}_{k|k}\right] \tag{10}$$

where $\hat{\boldsymbol{f}}^{\mathrm{u}}_{k|k}$ denotes the estimation of $\boldsymbol{f}^{\mathrm{u}}_k$ and $\boldsymbol{K}_{\theta,k}$ is the Kalman gain matrix for the estimation of parameter vector $\boldsymbol{\theta}$ given by

$$\boldsymbol{K}_{\theta,k} = \boldsymbol{P}_{\theta,k|k-1}\boldsymbol{H}^{T}_k\left(\boldsymbol{H}_k\boldsymbol{P}_{\theta,k|k-1}\boldsymbol{H}^{T}_k + \boldsymbol{R}_k\right)^{-1} \tag{11}$$

The error covariance matrix $\boldsymbol{P}_{\theta,k+1|k}$ is recursively estimated by

$$\boldsymbol{P}_{\theta,k|k-1} = (\boldsymbol{I} - \boldsymbol{K}_{\theta,k}\boldsymbol{H}_k)\boldsymbol{P}_{\theta,k-1|k-2} \tag{12}$$

2.1.2 Step-two: estimation of the structural state vector

In step-two, the state vector is updated by the Kalman estimator based on the state equation of Eq. (2) and the observation equation of Eq. (3) as

$$\hat{\boldsymbol{X}}_{k+1|k} = \tilde{\boldsymbol{X}}_{k+1|k} + \boldsymbol{K}_{X,k}\left[\boldsymbol{y}_k - \boldsymbol{h}\left(\hat{\boldsymbol{X}}_{k|k-1},\hat{\boldsymbol{\theta}}_k,\boldsymbol{f}_k\right) - \boldsymbol{B}^{\mathrm{u}}\hat{\boldsymbol{f}}^{\mathrm{u}}_{k|k}\right] \tag{13}$$

where $\tilde{\boldsymbol{X}}_{k+1|k}$ is the predicted state vector $\boldsymbol{X}_{k+1}$ which can be obtained by integration of Eq. (2) as

$$\tilde{\boldsymbol{X}}_{k+1|k} = \hat{\boldsymbol{X}}_{k|k-1} + \int_{k\Delta t}^{(k+1)\Delta t} g\left(\hat{\boldsymbol{X}}_{t|k},\hat{\boldsymbol{\theta}}_k,\boldsymbol{f},\hat{\boldsymbol{f}}^{\mathrm{u}}_{k|k}\right)dt \tag{14}$$

$\boldsymbol{K}_{X,k}$ is the Kalman gain matrix for state vector $\boldsymbol{X}$ given by

$$\boldsymbol{K}_{X,k} = \boldsymbol{\Phi}_{X,k}\boldsymbol{P}_{X,k|k-1}\boldsymbol{H}^{T}_{X,k}\left(\boldsymbol{H}_{X,k}\boldsymbol{P}_{X,k|k-1}\boldsymbol{H}^{T}_{X,k} + \boldsymbol{R}_k\right)^{-1} \tag{15}$$

$\boldsymbol{\Phi}_{X,k}$ is the state transition matrix which has the following form

$$\boldsymbol{\Phi}_{X,k} = \boldsymbol{I} + \Delta t \cdot \left[\frac{\partial \mathrm{g}(\boldsymbol{X},\boldsymbol{\theta},\boldsymbol{f},\boldsymbol{f}^{\mathrm{u}})}{\partial \boldsymbol{X}}\right]_{X=\hat{X}_{k|k-1},\theta=\hat{\theta}_k} \tag{16}$$

and the error covariance matrix $\boldsymbol{P}_{X,k+1|k}$ is recursively estimated by

$$\boldsymbol{P}_{X,k+1|k} = \boldsymbol{\Phi}_{X,k}\boldsymbol{P}_{X,k|k-1}\boldsymbol{\Phi}^{T}_{X,k} - \boldsymbol{K}_{X,k}\boldsymbol{H}_{X,k}\boldsymbol{P}_{X,k|k-1}\boldsymbol{\Phi}^{T}_{X,k} + \boldsymbol{Q}_k \tag{17}$$

2.2 Stage-two: Identification of the unknown excitations

After the recursive estimation of the state vector and structural parameters by the proposed two-step Kalman estimator in stage-one, the unknown excitations can be estimated by the least-squares estimation in stage-two.

Under the conditions: i) the number of output measurements is greater than that of the unknown excitations, and ii) measurements (sensors) are available at the DOFs where the external excitation vector $\boldsymbol{f}^{\mathrm{u}}$ acts, i.e., matrix $\boldsymbol{B}^{u}$ in Eq. (3) is non-zero; the unknown external excitations at time $t = (\mathrm{k}+1)\times \Delta t$ can be estimated by least -squares estimation as

$$\hat{\boldsymbol{f}}^{\mathrm{u}}_{\mathrm{k}+1|\mathrm{k}+1} = [(\boldsymbol{B}^{\mathrm{u}})^{T}\boldsymbol{B}^{\mathrm{u}}]^{-1}(\boldsymbol{B}^{\mathrm{u}})^{T}\left\{\boldsymbol{y}_{\mathrm{k}+1} - \boldsymbol{h}\left(\hat{\boldsymbol{X}}_{\mathrm{k}+1|\mathrm{k}}, \hat{\boldsymbol{\theta}}_{\mathrm{k}|\mathrm{k}}, \boldsymbol{f}_{\mathrm{k}+1}\right)\right\} \tag{18}$$

where $\hat{\boldsymbol{f}}^{\mathrm{u}}_{\mathrm{k}+1|\mathrm{k}+1}$ is the estimation of $\boldsymbol{f}^{\mathrm{u}}_{k+1}$.

3. Numerical example validations of the proposed algorithm

To validate the effectiveness of the proposed algorithm, several numerical simulation examples are used in this paper.

3.1 The phase I IASC–ASCE SHM benchmark building under unknown excitation

A benchmark building for SHM was established by the IASC-ASCE for comparing various system identification and damage detection techniques (Bernal and Beck 2004, Johnson *et al.* 2004). In the benchmark problem, several cases with different damage patterns are presented. The complex case 6 as shown in Fig. 1(a) is considered in this paper. In case 6, the three-dimension (3D) building model with asymmetric mass at the top floor is subjected to an external force applied on the diagonal of the top floor and the number of measured acceleration response is limited (sensors only deployed on the 2nd and 4th floors). Rayleigh damping assumption is employed and the damping matrix is assumed as

$$\boldsymbol{C} = \alpha\boldsymbol{M} + \beta\boldsymbol{K} \tag{18}$$

where α and β are two Rayleigh damping coefficients which depend on structural damping ratios and frequencies. In this benchmark building, the corresponding damping ratios are assumed as 1%.

Since the benchmark building model is three-dimension, the structural state consists of the displacement and velocity response at each floor level in the *x*, *y* and rotational directions, respectively. The unknown structural parametric vector is $\boldsymbol{\theta} = (k_1, k_2, \cdots, k_{16}, \alpha, \beta)^T$ as shown in Fig. 1(b). The external force applied at the top floor is assumed unknown. The first four damage patterns in the benchmark problem are studied herein as shown in Fig. 1(a), i.e., damage patterns include damage pattern 1 (DP1): all braces in the first story are removed, damage pattern 2 (DP2): all braces in both the 1st and 3rd floors are removed, damage pattern 3 (DP3): one brace is removed in the 1st story, and damage pattern 4 (DP4): one brace is removed in each of the 1st and 3rd stories. To consider the influence of measurement noise, structural acceleration responses are superimposed with the corresponding white noise with 2% noise- to- signal ratio in root mean square (rms). The initial guess of the structural parameters are selected with 30% bias with their actual values and the initial values for the state variables are zero.

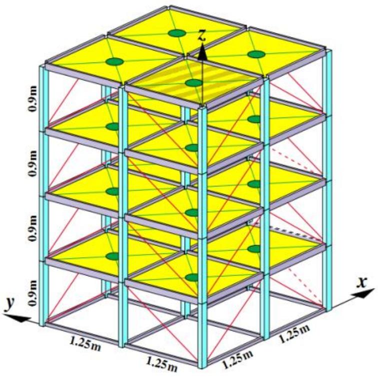

(a) The configuration of the benchmark building model

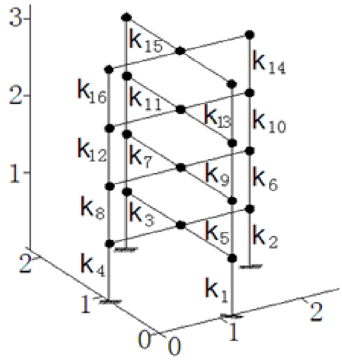

(b) 3D building model with 12 DOFs

Fig. 1 The Phase-I IASC-ASCE Benchmark building model for SHM

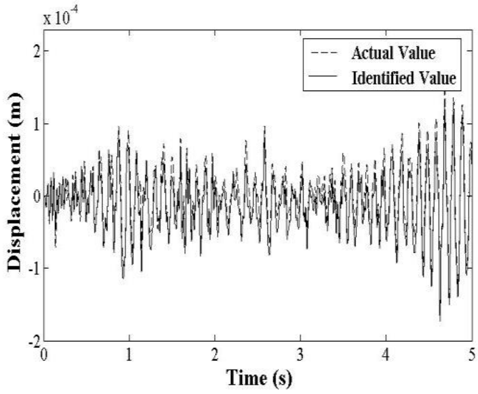

(a) Displacement responses in x-direction of the 1st floor (DP1)

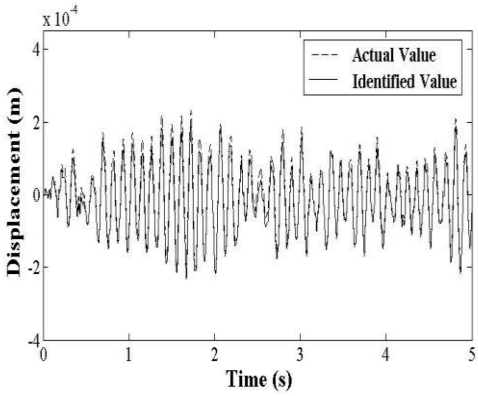

(b) Displacement responses in y-direction of the 3rd floor (DP4)

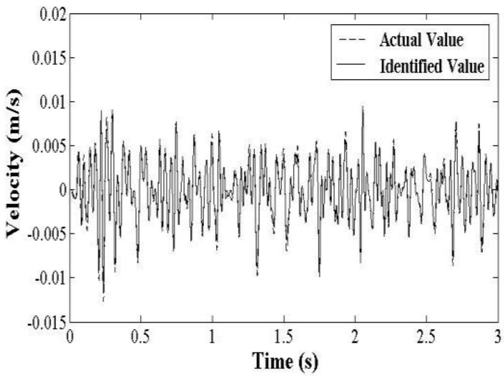

(c) Velocity responses in x -direction of the 1st floor (DP3)

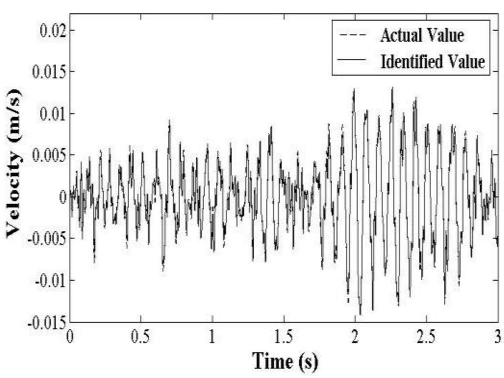

(d) Velocity responses in *x*-direction of the 3rd floor (DP4)

Fig. 2 Comparisons of identification results with actual values

In Figs. 2(a)-2(d), the identified displacement and velocity responses (in solid curves) are compared with their corresponding actual values (in dashed curves). The convergences of the identified element stiffness k_1 and k_2 of the building in damage pattern 1 are shown in Figs. 3(a) and 3(b). It is noted that the identified stiffness parameters converge quite fast. Then, the identified external excitation is compared with its actual value in Fig. 4. From the above comparisons, it is observed that the proposed algorithm can accurately identify structural responses, structural parameters as well as the unknown external excitation even though the sensors are only deployed on the 2nd and 4th floors of the building model.

In Tables 1-1 and 1-2, the identified stiffness parameters of the benchmark building in undamaged, damage pattern1 (DP1), damage pattern 2 (DP2), damage pattren3 (DP3), and damage pattern 4 (DP4) are summarized and compared with their corresponding actual values, respectively. It is demonstrated that the proposed algorithm can identify all structural stiffness parameters with good accuracy and detect structural damage based on the reduction of the identified stiffness parameters as indicated by the values in bold face in these two tables. However, the identification accuracy decrees when the measurement noise level increases.

Table1-1 Comparisons of stiffness parameters in the benchmark model (DP1 and DP2)

Stiffness	Undamaged			Damage Pattern 1			Damage Pattern 2		
	Actual (MN/m)	Identified (MN/m)	error (%)	Actual (MN/m)	Identified (MN/m)	Stiffness reduction (%)	Actual (MN/m)	Identified (MN/m)	Stiffness reduction (%)
k_1	53.3	55.1	3.45	**29.2**	**29.7**	**-44.28**	**29.2**	**30.3**	**-43.11**
k_2	34.0	33.8	-0.49	**9.84**	**10.2**	**-70.07**	**9.84**	**10.2**	**-70.09**
k_3	53.3	54.9	2.98	**29.2**	**28.8**	**-45.89**	**29.2**	**30.1**	**-43.58**
k_4	34.0	34.4	1.14	**9.84**	**9.11**	**-73.34**	**9.84**	**10.1**	**-70.36**
k_5	53.3	51.8	-2.85	53.3	53.1	-0.40	53.3	50.5	-5.22
k_6	34.0	33.3	-2.20	34.0	33.2	-2.34	34.0	34.2	0.57
k_7	53.3	51.5	-3.29	53.3	53.4	0.20	53.3	51.1	-4.29
k_8	34.0	34.8	2.23	34.0	34.9	2.59	34.0	33.5	-1.44
k_9	53.3	51.3	-3.70	53.3	50.7	-4.84	**29.2**	**28.1**	**-47.24**
k_{10}	34.0	34.4	1.25	34.0	34.1	0.31	**9.84**	**9.72**	**-71.50**
k_{11}	53.3	51.4	-3.61	53.3	52.8	-1.00	**29.2**	**28.5**	**-46.61**
k_{12}	34.0	34.5	1.32	34.0	33.8	-0.63	**9.84**	**9.71**	**-71.56**
k_{13}	53.3	53.0	-0.53	53.3	54.6	2.39	53.3	52.0	-2.40
k_{14}	34.0	34.6	1.69	34.0	33.2	-2.47	34.0	34.3	0.87
k_{15}	53.3	53.6	0.58	53.3	55.0	3.13	53.3	53.3	0.06
k_{16}	34.0	33.7	-1.02	34.0	35.6	4.59	34.0	33.9	-0.26

Table1-2 Comparisons of stiffness parameters in the benchmark model (DP3 and DP4)

Stiffness	Damage Pattern 3			Damage Pattern 4		
	Actual (MN/m)	Identified (MN/m)	Stiffness reduction (%)	Actual (MN/m)	Identified (MN/m)	Stiffness reduction (%)
k_1	53.3	54.2	1.64	53.3	52.8	-0.91
k_2	**21.9**	**22.2**	**-34.69**	**21.9**	**22.6**	**-33.60**
k_3	53.3	52.9	-0.76	53.3	53.1	-0.46
k_4	34.0	33.8	-0.63	34.0	33.2	-2.22
k_5	53.3	53.3	-0.03	53.3	54.7	2.69
k_6	34.0	34.3	0.94	34.0	32.8	-3.45
k_7	53.3	55.2	3.49	53.3	53.1	-0.30
k_8	34.0	33.8	-0.66	34.0	34.0	0.10
k_9	53.3	51.8	-2.81	**41.2**	**40.9**	**-23.36**
k_{10}	34.0	34.1	0.33	34.0	34.4	1.24
k_{11}	53.3	51.8	-2.74	53.3	50.9	-4.58
k_{12}	34.0	34.2	0.54	34.0	34.6	1.85
k_{13}	53.3	52.8	-0.97	53.3	53.3	0.08
k_{14}	34.0	34.4	1.11	34.0	33.6	-1.22
k_{15}	53.3	53.3	-0.06	53.3	54.4	2.10
k_{16}	34.0	34.1	0.39	34.0	34.8	2.31

3.2 A high-rise shear building under unknown excitation

In order to validate the performances of proposed algorithm in dealing with a large number of unknown parameters, identification of structural damage of a 30-story high-rise shear building under unknown excitation is selected an example. The mass of the building model is concentrated on the floor level and set to be 60 kg for each floor, the value of story stiffness is $1.2*10^5$ N/m for each floor and the corresponding viscous damping value of each floor is 200 N*s/m. An unknown external excitation is applied at the top floor of the building. It is assumed that only 18 accelerometers are deployed at the 1st, 3nd, 5th, 7th, 10th, 12th, 14th, 17th, 19th, 21th, 23th, 25th, 27th, 29th, 20th floor, respectively and the theoretical computed acceleration responses are also superimposed by the corresponding white noise with 2% noise- to- signal ratio in rms.

In this example, the number of unknown parameters is 60 and the size of extended state vector is 120. However, the proposed algorithm can identify the structural parameters, state vector and the unknown external excitation in a two-stage and two-step approach. The initial guess of the structural parameters are selected as: story stiffness $k_{i,0}$ =0.8*105 N/m ; $c_{i,0}$ =150 N*s/m. (i=1,2,…16). The initial values for the state variables are assumed zero.

Table 2-1 gives the comparisons between the identification results of story stiffness and the corresponding actual values. Table 2-2 shows the similar comparisons for the damping parameters. The identified external excitation is shown in Fig. 5 with comparison to its actual value. From these comparisons, it is shown that the proposed algorithm can identify unknown structural parameters and excitation with satisfied accuracy for a structure with a large number of unknown parameters. However, the identification accuracy is also influenced by the level of measurement noise.

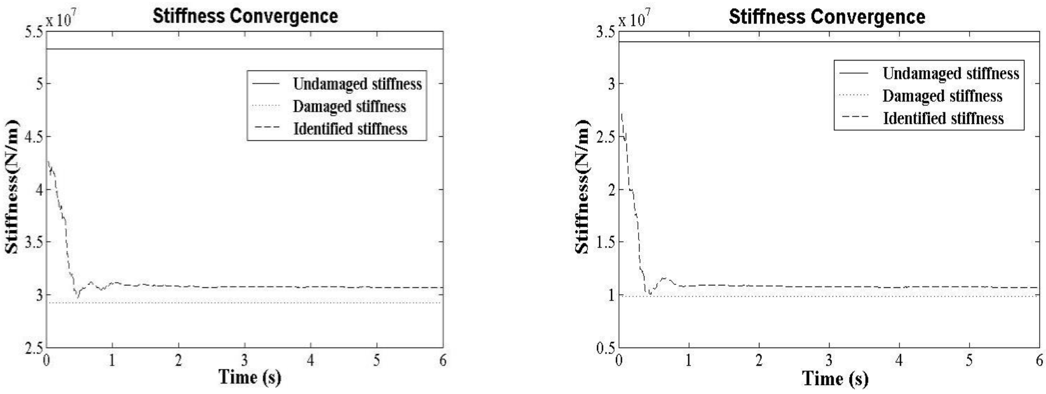

(a) Convergences of identified k_1 (b) Convergences of identified k_2

Fig. 3 Convergences of identified stiffness parameters (DP1)

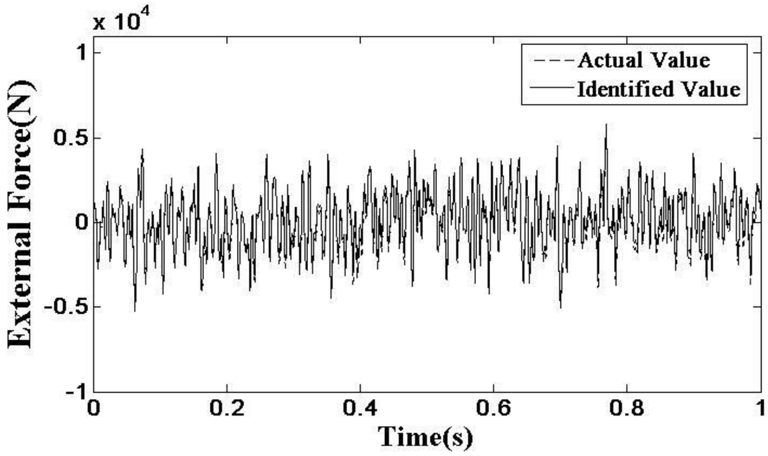

Fig. 4 Comparison of the identified excitation and the actual one on the benchmark model

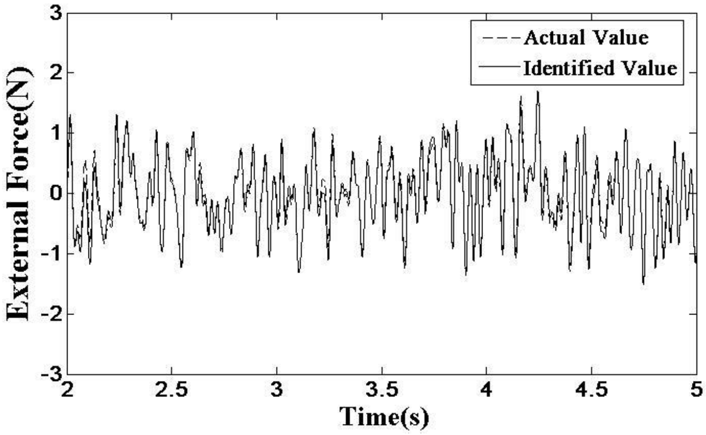

Fig. 5 Comparison of the identified excitation and the actual one on the shear building model

Table 2-1 Comparisons of story stiffness in the high-rise shear building

Stiffness parameters	Actual (10^5N/m)	Identified (10^5N/m)	Error (%)	Stiffness parameters	Actual (10^5N/m)	Identified (10^5N/m)	Error (%)
k_1	1.20	1.18	-1.34	k_{16}	1.20	1.20	0.11
k_2	1.20	1.20	0.17	k_{17}	1.20	1.18	-1.31
k_3	1.20	1.21	0.45	k_{18}	1.20	1.20	0.31
k_4	1.20	1.22	1.39	k_{19}	1.20	1.19	-1.03
k_5	1.20	1.21	1.01	k_{20}	1.20	1.21	1.13
k_6	1.20	1.20	-0.06	k_{21}	1.20	1.20	0.07
k_7	1.20	1.20	-0.32	k_{22}	1.20	1.20	0.19
k_8	1.20	1.21	0.45	k_{23}	1.20	1.23	2.11
k_9	1.20	1.21	0.46	k_{24}	1.20	1.20	-0.35
k_{10}	1.20	1.19	-0.71	k_{25}	1.20	1.20	0.10
k_{11}	1.20	1.20	0.09	k_{26}	1.20	1.19	-0.94
k_{12}	1.20	1.21	0.72	k_{27}	1.20	1.19	-1.14
k_{13}	1.20	1.22	1.31	k_{28}	1.20	1.19	-0.59
k_{14}	1.20	1.20	-0.09	k_{29}	1.20	1.20	0.22
k_{15}	1.20	1.21	0.61	k_{30}	1.20	1.22	2.02

Table 2-2 Comparisons of damping parameters in the high-rise shear building

Damping parameters	Actual (N*s/m)	Identified (N*s/m)	Error (%)	Damping parameters	Actual (N*s/m)	Identified (N*s/m)	Error (%)
c_1	200	191.4	-4.32	c_{16}	200	192.4	-3.78
c_2	200	198.6	-0.68	c_{17}	200	192.7	-3.64
c_3	200	202.7	1.37	c_{18}	200	192.9	-3.55
c_4	200	205.8	2.88	c_{19}	200	192.1	-3.95
c_5	200	206.8	3.42	c_{20}	200	196.8	-1.59
c_6	200	198.2	-0.88	c_{21}	200	200.8	0.39
c_7	200	192.9	-3.56	c_{22}	200	204.9	2.44
c_8	200	194.9	-2.55	c_{23}	200	206.2	3.12
c_9	200	191.2	-4.40	c_{24}	200	199.7	-0.17
c_{10}	200	195.9	-2.06	c_{25}	200	199.1	-0.45
c_{11}	200	195.6	-2.22	c_{26}	200	190.5	-4.77
c_{12}	200	206.6	3.29	c_{27}	200	197.9	-1.04
c_{13}	200	208.1	4.07	c_{28}	200	197.0	-1.50
c_{14}	200	197.4	-1.30	c_{29}	200	209.0	4.51
c_{15}	200	196.6	-1.69	c_{30}	200	211.6	5.81

3.3 A large size plan truss under unknown excitation

To validate the proposed algorithm for damage detection of other types of structures, a large size plane truss is selected as an example. As shown in Fig. 6, the plane truss consisting of 23 bars is subjected to an unmeasured external excitation. All the bar elements have the same cross-section area A = 8.947×10^{-5} m^2, mass density ρ = 7850 kg/m^3 and the Young's module E = 2×10^7 Pa. The length of each horizontal bar is 2m while it is $\sqrt{2}$ m for each inclined bar. In the finite element model, the structural global mass matrix $\boldsymbol{M}$ and global stiffness matrix $\boldsymbol{K}$ can be formulated by the assemblage of each element mass matrix and element stiffness matrix, in which the stiffness parameter of the *i*-th element is defined as $k_i = EA/l_i$. Rayleigh damping is employed with structural damping ratios assumed as $\xi_1 = \xi_2 = 0.03$ for the first and second modes.

In this numerical example, it is assumed that the vertical acceleration responses at nodes 1, 2 and 4, and the lateral acceleration responses at nodes 6, 7, 8, 9, 10, 11, 12 are not observed. All the calculated acceleration responses are polluted by white noise with 2% noise-to-signal ratio in rms. Assumed that structural damage occurs in bar element 9 and element 17. The proposed algorithm is utilized to identify structural parameters as well as the unknown excitation. The initial guess of the structural parameters are selected with 30% bias with their actual values and the initial values for the state variables are assumed zero.

The identification results of equivalent element stiffness are shown in Table 3 and compared with those of actual values. It is demonstrated that the proposed algorithm is capable of detecting and localizing structural damage from the reductions of the identified equivalent element stiffness parameters as indicated by the values in bold faces in Table 3. Fig. 7 shows the identified unknown excitation which is in close agreement with the actual excitation.

Table 3 Comparisons of truss element stiffness parameters

Element stiffness (N/m)	Undamaged (Actual)	Undamaged (Identified)	Error(%)	Damaged (Actual)	Damaged (Identified)	Error(%)
k_1	1265.4	1257.5	-0.62	1265.4	1258.9	-0.51
k_2	894.8	886.0	-0.98	894.8	883.6	-1.25
k_3	1265.4	1271.0	0.44	1265.4	1274.7	0.74
k_4	894.8	889.8	-0.56	894.8	889.2	-0.63
k_5	1265.4	1248.2	-1.35	1265.4	1252.8	-1.00
k_6	894.8	902.6	0.88	894.8	896.5	0.20
k_7	1265.4	1257.8	-0.60	1265.4	1261.7	-0.29
k_8	894.8	909.1	1.60	894.8	874.1	-2.31
k_9	1265.4	1266.0	0.05	**885.8**	**886.9**	0.12
k_{10}	894.8	892.4	-0.27	894.8	886.1	-0.97
k_{11}	1265.4	1266.9	0.12	1265.4	1259.9	-0.43
k_{12}	894.8	924.5	3.32	894.8	878.8	-1.78
k_{13}	1265.4	1255.8	-0.75	1265.4	1269.5	0.32
k_{14}	894.8	897.2	0.28	894.8	893.6	-0.13
k_{15}	1265.4	1264.6	-0.06	1265.4	1267.6	0.18
k_{16}	894.8	906.2	1.28	894.8	865.3	-3.29
k_1	1265.4	1272.9	0.60	1265.4	1279.1	1.09
k_{17}	894.8	895.7	0.11	**626.4**	**611.2**	-2.43
k_{18}	1265.4	1250.9	-1.14	1265.4	1254.6	-0.85
k_{19}	894.8	896.0	0.14	894.8	921.6	2.99
k_{20}	1265.4	1252.2	-1.05	1265.4	1245.5	-1.57
k_{21}	894.8	891.1	-0.41	894.8	917.7	2.56
k_{22}	1265.4	1237.5	-2.21	1265.4	1250.8	-1.15

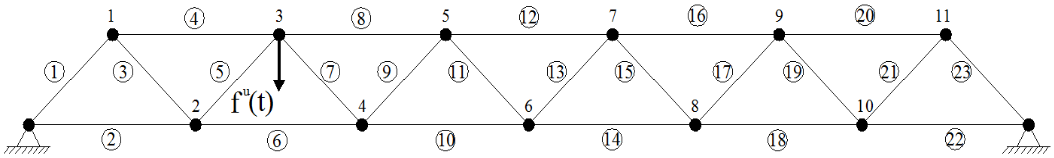

Fig. 6 A large size plan truss subject to an unknown excitation

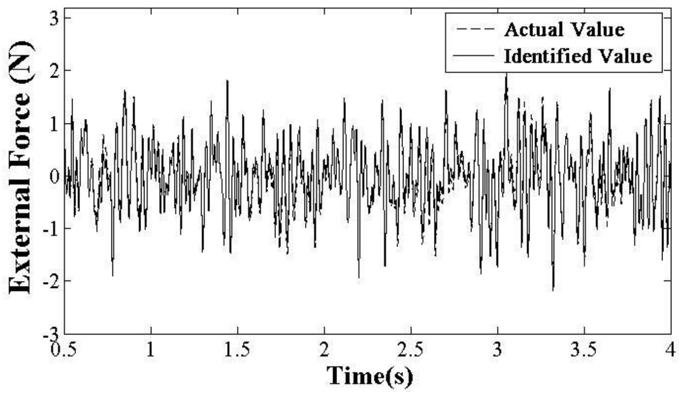

Fig. 7 Comparison of the identified excitation and the actual one on the truss

4. Experimental validations of the proposed algorithm

To further validate the feasibility of the proposed algorithm, two lab experimental tests on the identification of structural damage and unknown external excitations are used in this paper. Also, an experimental demonstration of intelligent structural damage detection of a lab multi-story model based on smart sensors embedded with the proposed algorithm is studied.

4.1 A frame structure with joint damage under shake table test

It has been shown that beam-column joints in a frame structure are more susceptible to damage than the other members of the structure under severe excitation such as strong earthquakes (Li *et al.* 2007, Karayannis *et al.* 2011, Zhang and Han 2013). But there are only a few studies on the identification of beam-column joint damage (Chen 2008, Weng *et al.* 2009, Katkhudat *et al.* 2010, Xia 2011, Xu *et al.* 2012). Since the performances of the joints are critical factors in many structural damages or collapses, it is necessary to investigate efficient methods for damage identification of frame structures with joint damage under earthquake excitation. However, damage detection of a frame structure with joint damage involves the identification of more unknown structural parameters due to the unknown joint connection stiffness in addition to those of the beam and column element stiffness, which needs algorithms that can overcome the drawbacks of conventional EKF approaches.

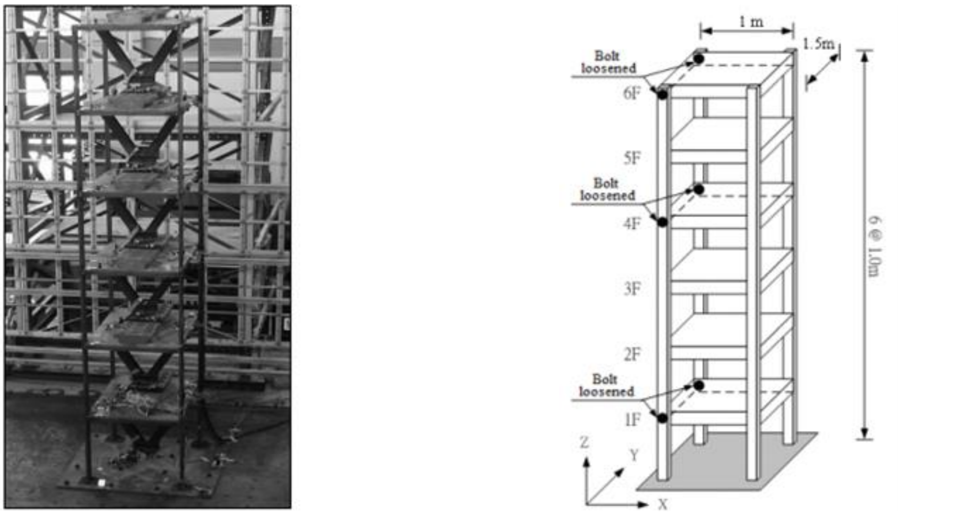

(a) Photo of the frame (b) FE model with locations of joint damage

Fig. 8 Experimental test of a six-story steel frame with joint damage from Weng *et al*. (2009)

In this paper, the experimental data of the shake table test of a 1/3-scaled 6-story steel frame structure with loosened bolts (Weng et *al.* 2009, Xia 2011) are used. As shown in Figs. 8(a) and 8(b), the frame model in the lab is a symmetric single bay six-story structure (Weng *et al.* 2009). The constructions of connections are: (i) beam-floor is welded connection, and (ii) column-beam, bracing-floor and structure-shake table are bolted connections. A joint of the frame is considered as semi-rigid connection which is modeled as a zero-length rotational spring with rotational stiffness parameter γ and joint damage is represented by the reduction of beam-column connection rigidity parameter γ. More details can be found in the Ph. D dissertation of Xia (2011). The mass on each floor lumped mass is 862.85 kg. Structural damping is assumed as Rayleigh damping. The method of static condensation is used to reduce the number of degrees of freedom of the finite-element model, whereas the same number of unknown structural parameters in the original complex structure has been retained in the reduced-order system. This approach not only reduces the number of required sensor measurements but also removes response quantities which are difficult to measure, such as the rotational acceleration of a nodal point (Weng et *al.* 2009, Xia 2011). Based on the static condensation, the reduced-order FE model of the fame is a 6-DOF symmetric structure with a total of 21 unknown structural stiffness vector given by $\boldsymbol{\theta} = [k_{b1}, k_{b2}, ..., k_{b6}, k_{c1}, k_{c2}, ..., k_{c6}, \gamma_0, \gamma_1, ..., \gamma_6, \alpha, \beta]$, in which k_{bi} and k_{ci}, (i=1,2,…,6) are the equivalent element stiffness parameters of the i-th beams and columns, respectively, γ_0 is the rotational stiffness parameter of the column connected to the ground, and γ_i (1=1,2,…,6) is the rotational spring stiffness of the beam-column joints at the i-th floor (Weng et *al.* 2009, Xia 2011).

It is difficult to measure the dynamic responses rotational angles in frame structures. In this paper, accelerometers installed on each floor for the lateral acceleration responses are used while the base excitation of the shake table is assumed unknown. The sampling frequency of the measurements is 200 Hz. Some patterns of joint damage scenarios are artificially introduced (bolt loosened at different levels of floor) as shown in Fig. 8(b) where black dots indicate the locations of bolt loosening. Two damage patterns are considered in this paper as follows:

Damage pattern 1 (DP1): bolts loosened on1st floor;

Damage pattern 2 (DP2): bolts loosened on both 1st and 4th floors;

Table 4 shows the identification results of structural stiffness parameters for the undamaged and damage patterns 1-2. From the reductions of the identified joint stiffness (rotational stiffness) indicated by the values in bold faces in the table, the locations and degrees of joint damage in the frame can be detected.

Table 4 Identification results of stiffness parameters of the experimental 6-story frame

Stiffness Parameters	Identified Stiffness Parameters				
	Undamaged	Damage Pattern 1	Stiffness Degradation	Damage Pattern 1	Stiffness Degradation
k_{b1}(kN/m)	839	779	7.2%	763	9.1%
k_{b2}(kN/m)	808	741	8.3%	749	7.2%
k_{b3}(kN/m)	790	726	8.1%	767	2.8%
k_{b4}(kN/m)	728	738	-1.4%	764	-5.0%
k_{b5}(kN/m)	739	801	-8.4%	800	-8.4%
k_{b6}(kN/m)	807	828	-2.6%	804	0.3%
k_{c1}(kN/m)	71.9	76.4	-6.3%	75.2	-4.7%
k_{c2}(kN/m)	82.1	78.8	3.9%	76.2	7.2%
k_{c3}(kN/m)	77.9	80.1	-2.9%	82.1	-5.4%
k_{c4}(kN/m)	79.3	80.2	-1.2%	76.0	4.0%
k_{c5}(kN/m)	72.6	73.9	-1.9%	75.0	-3.3%
k_{c6}(kN/m)	87.8	90.1	-2.6%	85.9	2.2%
γ_0	12.8	11.9	6.3%	13.8	-7.8%
γ_1	0.38	**0.16**	**59.4**%	**0.15**	**60.5**%
γ_2	0.46	0.43	6.5%	0.43	6.5%
γ_3	0.62	0.58	6.4%	0.59	4.8%
γ_4	0.56	0.55	1.5%	**0.16**	**72.1**%
γ_5	0.74	0.79	-6.8%	0.78	-5.4%
γ_6	0.88	0.91	-3.1%	0.89	-1.2%

4.2 A multi-story shear frame model under unknown excitation

Identification of structural damages of an 8-storey shear frame model as well as the unknown excitation in lab experiment is studied. As shown in Fig. 9(a), the 8-storey frame model with 1.6 m tall and 0.35 m*0.25 m in plan behaves as a lumped mass shear frame. A magnetic shaker induces external excitation to the model at the 3rd story level which is installed a force transducer to record the excitation force. 6 light PCB accelerometers are deployed on the 1st, 3rd, 5th, 6th, 7th and 8th floors to measure the acceleration responses at the corresponding floor levels as shown in Fig. 9(b). The sampling frequency is 1 kHz for all measured data. Fig. 10(a) gives the details about the connection between floors and columns. Structural damage is simulated by replacing the flexible columns with thinner ones as shown in Fig. 10(b), which results in the reduction of corresponding story stiffness. In this experiment, structural damage is assumed to occur in the 6th story by replacing the four columns with thinner ones, which leads to the reduction of k_6. The initial guess of the structural parameters are selected as $k_{i,0}$ =100kN/m (i=1,2,…,8) and the initial values for the state variables are assumed zero.

Figs. 11(a) and 11(b) show the convergences of the identified floor k_2 and k_6 of the undamaged building (in dashed curves) and the damaged building (in solid curves), respectively. It is noted that the identified stiffness parameters converge quite fast. Fig. 12 shows the identified unknown external excitation to the undamaged frame model, which is close to the actual excitation recorded by the force transducer. In Table 5, the identification results of story stiffness of the undamaged and damaged frame model are shown in the 2nd and 3rd columns, respectively. From the relative change of identified story stiffness indicated by value in bold face in the 4th column in Table 5, it is clearly shown that the proposed algorithm can detect structural damage of the frame model.

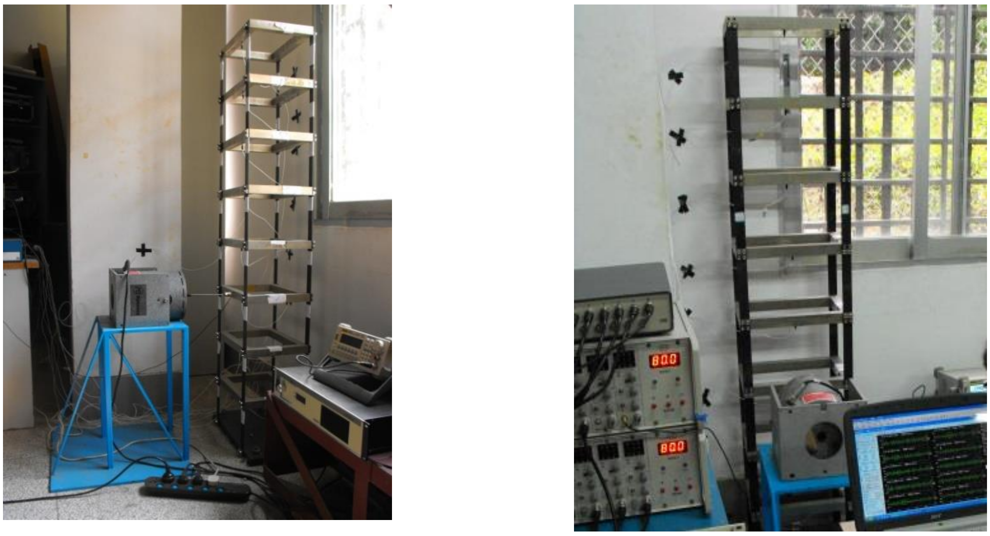

(a) The eight-story lab shear frame model (b) Data acquisition during the experiment

Fig. 9 Experimental study with an eight-storey building model

Table 5 Identified story stiffness of the experimental multi-story frame

Story	Stiffness [kN/m]		Relative Change
	Undamaged	Damaged	
1st	123.04	124.34	1.06%
2nd	134.97	132.02	-2.19%
3rd	129.66	135.25	4.31%
4th	131.10	128.80	-1.75%
5th	133.77	131.96	-1.37%
6th	132.81	79.96	**-39.79%**
7th	130.29	131.83	1.18%
8th	130.96	130.46	-0.38%

(a) The installation of the PCB accelerometers (b) Two types of columns

Fig. 10 Beams and columns of the shear building model

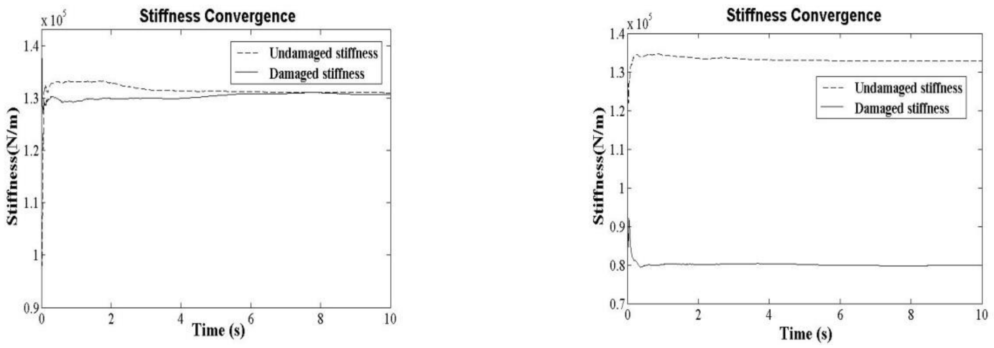

(a) Convergence of identified stiffness k_2 (b) Convergence of identified stiffness k_6

Fig. 11 Convergences of identified floor stiffness

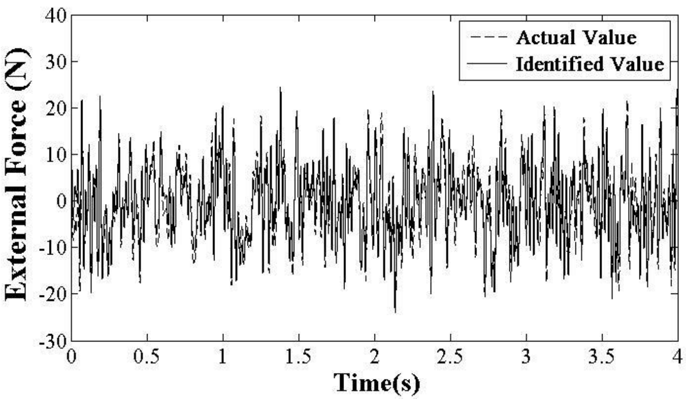

Fig. 12 Comparison of the identified excitation and the actual one on the lab shear frame model

4.3 A demonstration of intelligent structural damage detection with the proposed algorithm

Based on the proposed algorithm of two stage and two-step approach, computational effort and storage requirements are greatly reduced compared with the conventional EKF approaches. This reduction may be not remarkable for a current advanced computer which has strong computing processor unit and large storage capacities, but it is significant for intelligent structural identification and damage detection implemented by smart sensors in which the micro-processors have limited computational power and storage capacities. To demonstrate the superiorities of the proposed algorithm, the proposed algorithm is embedded into the micro-processor of smart sensors in a wireless sensor network (WSN) developed by the authors (Lei *et al.* 2011). The designed WSN has a two-level cluster-tree architecture in which distributed sensors are grouped into clusters and a cluster head is assigned to each cluster to coordinate the sensors. The cluster head contains a low power digital signal processor (DSP) with strong computing capacity. Thus, the WSN provides distributed computation resources at group level, which is useful for the implementation of computational algorithms for structural health monitoring. Some lab and in field experiment tests on the accuracy of data acquisition, time synchronization of measurement data and other capabilities of the wireless sensor units validated that the designed wireless sensor network possesses favorable performances of data collection, transmission and distributed computation (Lei *et al.* 2011).

In this paper, based on the experimental test of the proposed algorithm on the multi-story shear frame under unknown excitation in Sect. 4.2, a lab experimental test is conducted to demonstrate the structural identification and damage detection implemented by the smart sensor network embedded with the proposed algorithm. As shown in Fig. 13, six sensor nodes connected with PCB accelerometers are installed at the 2nd, 3rd, 4th, 5th 6th and 8th floors to collect acceleration responses, respectively. It is assumed that the two flexible columns in the 5th story were replaced by thinner ones to simulate structural damage. To further reduce the compotation effort and storage requirement, substructural identification approach is adapted (Lei *et al*. 2013). The frame model is divided into two substructures with floors 1-4 being the 1st substructure and floors 5-8 being the second one. The upper substructure is subject to the measured acceleration $\ddot{x}_4(t)$ while the lower substructure is excited by both the interface force and the unknown excitation. In each substructure, the deployed sensor nodes are grouped into a cluster. Each cluster is assigned with a cluster head (ch) to collect data from the sensor nodes during vibration. Final identification results of story stiffness parameters and the unknown external excitation are sent to the central server (PC). Figs. 14(a) and (b) show the identified story stiffness parameters of the undamaged and damaged frame models on the screen of the PC server, in which Fig. 14(a) shows the two set of identification results on the screen of the PC server and Fig. 14(b) shows the zoom-in identification results on the screen of the PC server. To clearly illustrate the results, the identification results are summarized and compared in Table 6. By comparing these two set of identification results and the stiffness degradation values in the 4th column in the table, it is demonstrated that the proposed technique can autonomously detect and localize the structural damage by the large stiffness degradation value of the identified story stiffness k_5.

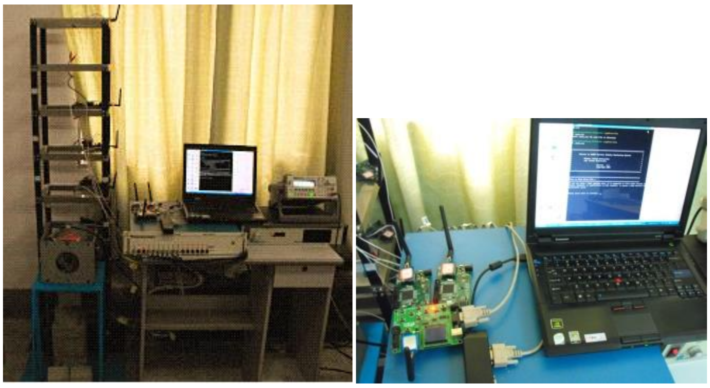

Fig. 13 Lab demonstration of intelligent damage detection based on WSN embedded with the proposed algorithm

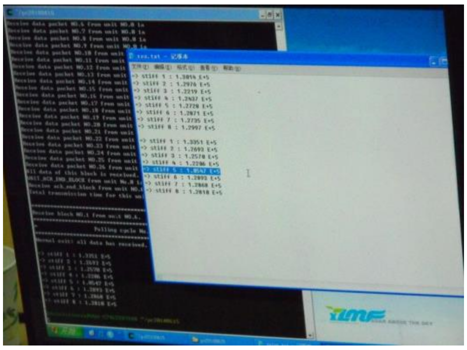

(a) Two set of identification results shown the screen of the PC server

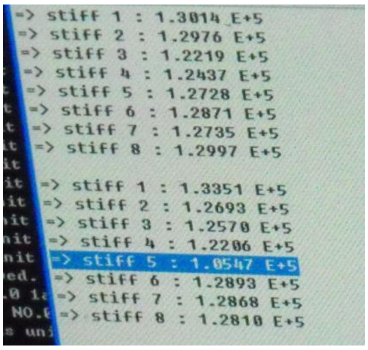

(b) Zoom-in identification results on the screen of the PC server

Fig. 14 Identification of story stiffness of the experimental frame model shown on PC screen

Table 6 Intelligent structural identification/damage detection results

Story Stiffness	Stiffness [kN/m]		Stiffness Degradation
	Undamaged	Damaged	
k_1	130.14	133.51	2.58%
k_2	129.76	126.93	-2.18%
k_3	122.19	125.70	2.87%
k_4	124.37	122.06	-2.86%
k_5	127.28	**105.47**	**-17.14%**
k_6	128.71	128.93	0.17%
k_7	127.35	128.68	1.04%
k_8	129.97	128.10	-0.38%

5. Conclusions

In this paper, an algorithm of a two stage and two-step approach is proposed for the identification of structural damage as well as unknown external excitations with partial measurements of structural acceleration responses. In stage-one, structural state vector and unknown structural parameters are recursively estimated by a two-step Kalman estimator approach, so the number of unknown variables to be estimated in each step is reduced. Then, the unknown excitations are recursively estimated sequentially by least-squares estimation in stage-two. Thus, structural identification and unknown excitation estimation are conducted sequentially. The proposed algorithm not only removes the drawbacks of the conventional EKF approach but also simplifies the identification problem and reduces computational efforts and storage requirements compared with other previous work. These superiorities are useful for intelligent structural damage detection due to the limited computational power and storage capacities of the micro-processors in smart sensors.

Several numerical simulation examples and lab experimental tests validate the effectiveness of the proposed algorithm for the identification of various structural damage patterns as well as unknown excitations. Also, a lab experimental test on a multi-story frame model demonstrates that the proposed algorithm can be embedded into the smart sensor network for intelligent structural damage detection.

The identification accuracies are influenced by the level of measurements noise; therefore, it is still necessary to improve the robustness of the proposed algorithm against high level measurement noises. Also, more numerical and experimental tests on complex structural configurations are needed to further validate the performances of the proposed algorithm, especially more experimental studies are required for the intelligent structural damage detection of complex structural systems.

Acknowledgments

This research is supported by the National Natural Science Foundation of China (NSFC) through Grant No.51178406, China National High Technology Research and Development Program 2007AA04Z420, and the research funding SLDRCE10-MB-01 from the State Key Laboratory for Disaster Reduction in Civil Engineering at Tongji University, China. The authors thank Prof. Chin-Hsiung Loh at National Taiwan University for his kind support of providing the experimental data of the shake table tests of a 1/3-scaled 6-story steel frame structure.

References

Azam, S.E. and Mariani S. (2007), “Unscented Kalman filtering for nonlinear structural dynamics”, *Nonlinear Dynam.*, **49**(1-2), 131-150;

Bernal, D. and Beck, J. (2004), “Special section: phase I of the IASC-ASCE structural health monitoring benchmark”, *J. Eng. Mech. - ASCE*, **130**(1), 1-127.

Chen, H.P. (2008), “Application of regularization methods to damage detection in large scale plane frame structures using incomplete noisy modal data”, *Eng. Struct.*, **30**(1), 3219-3227.

Fan, W. and Qiao, P.Z. (2011), “Vibration-based damage identification methods: A review and comparative study”, *Struct. Health Monit.*, **10**(1), 83-111.

Feng, M.Q. (2009), “Application of structural health monitoring in civil infrastructure”, *Smart Struct. Syst.*, **5**(4), 469-482.

Hoshiya, M. and Sutoh, A. (1993), “Kalman filter-finite element system method in identification”, *J. Eng. Mech. - ASCE*, **119**(2), 197-210.

Hsu, T.Y., Huang, S.K., Lu, K.C. Loh, C.H., Wang, Y. and Lynch, J.P. (2011), “On-line structural damage localization and quantification using wireless sensors”, *Smart Mater. Struct.*, **20**(10), 105025.

Huang, H.W., Yang, J.N. and Zhou L. (2010), “Adaptive quadratic sum-squares error with unknown inputs for damage identification of structures”, *Struct. Control Health Monit.*, **17**(4), 404-426.

Johnson, E.A., Lam, H.F., Katafygiotis, L.S. and Beck, J.L. (2004), “The phase I IASC–ASCE structural health monitoring benchmark problem using simulated data”, *J. Eng. Mech. - ASCE*, **130**(1), 3-15.

Julier, S., Uhlmann, J. and Durrant-Whyte, H.F. (2010), “A new method for the nonlinear transformation of means and covariances in filters and estimators”, *IEEE T. Automat. Contr.*, **45**(3), 477-482;

Karayannis, C.G., Favvata, M.J. and Kakaletsis, D.J. (2011), “Seismic behaviour of infilled and pilotis RC frame structures with beam-column joint degradation effect”, *Eng. Struct.*, **10**, 821-2831.

Katkhudat, H.N., Dwairi, H.M. and Shatarat, N. (2010), “System identification of steel framed structures with semi-rigid connections”, *Struct. Eng. Mech.*, **34**(3), 351-366.

Kim, J.H., Kim, K.Y. and Sohn, H. (2013), “Data-driven physical parameter estimation for lumped mass structures from a single point actuation test”, *J. Sound Vib.*, **332**(18), 4390-4402

Kim, J.H. and Lynch, J.P. (2012), “Subspace system identification of support-excited structures-part I: theory and black-box system identification”, *Earthq. Eng. Struct. D.*, **41**(15), 2235-2251.

Koh, C.G., See, L.M. and Balendra, T. (1991), “Estimation of structural parameters in time domain: a substructure approach”, *Earthq. Eng. Struct. D.*, **20**(8), 787-801.

Lee, K.J. and Yun, C.B. (2008), Parameter identification for nonlinear behavior of RC bridge piers using sequential modified extended Kalman filter. *Smart Structures and Systems*, **4**(3), 319-342.

Lei, Y., Jiang, Y.Q. and Xu, Z.Q. (2012), “Structural damage detection with limited input and output measurement signals”, *Mech. Syst. Signal Pr.*, **28**, 229-243.

Lei, Y., Lai, Z.L., Liu, L.J., Tan, Y.L. and Wang X. J. (2011), “A new type wireless sensor network for distributed structural damage detection”, *Proceedings of the 1st Middle East Conference on Smart Monitoring, Assessment and Rehabilitation of Civil Structures*, Feb. 8-10, Dubai UAE.

Lei, Y., Liu, C., Jiang. Y.Q. and Mao, Y.K. (2013), "Substructure based structural damage detection with limited input and output measurements", *Smart Struct. Syst.*, **12**(6), 619-640.

Li, G.Q., Shi, W.L. and Xiao Y. (2007), "State of the art of research on semi-rigid composite beam-to-column joints", *Progress Steel Build. Struct*., **9**(4), 11-22.

Li, J.C., Dackermann, U., Xu, Y.L. (2011), "Damage identification in civil engineering structures utilizing PCA-compressed residual frequency response functions and neural network ensembles", *Struct. Control Health Monit.*, **18**(2), 207-226.

Liu, X., Escamilla-Ambrosio, P.J. and Lieven, N.A. (2009), "Extended Kalman filtering for the detection of damage in linear mechanical structures", *J. Sound Vib.*, **325**, 1023-1046.

Lu Z.R. and Law, S.S. (2007), "Identification of system parameters and input force from output only", *Mech. Syst. Signal Pr*., 21(5), 2099-2111.

Lynch, J.P. (2007), "An overview of wireless structural health monitoring for civil structures", *Philos. T. R. Soc. A*, **365**, 345-372.

Mariani, S. and Ghisi, A. (2007), "Unscented Kalman filtering for nonlinear structural dynamics", *Nonlinear Dynam.*, **49**(1-2), 131-150;

Ou, J.P. and Li, H. (2010), "Structural health monitoring in mainland China: Review and future trends", *Struct. Health Monit.*, **9**(3), 219-231.

Park, J.W., Sim, S.H. and Jung, H.J. (2013), "Wireless sensor network for decentralized damage detection of building structures", *Smart Struct. Syst.*, **12**(3-4), 399-414.

Ren, W.X., Lin, Y.Q. and Fang, S.E. (2011), "Structural damage detection based on stochastic subspace identification and statistical pattern recognition: I. Theory", *Smart Mater. Struct.*, **20**(11),115009.

Sim, S.H., Spencer, B.F., Jr. and Zhang, M. (2010), "Automated decentralized modal analysis using smart sensors", *Struct. Control Health Monit.*, **17**(8), 872-894.

Sirca, Jr. G.F. and Adeli, H. (2012), "System identification in structural engineering", *Scientia Iranica A*., **19** (6), 1355-1364

Sohn, H., Farrar, C.R., Hemez, F.M., Shunk, D.D., Stinemates, D.W. and Nadler, B.R. (2003), *A review of structural health monitoring literature: 1996–2001*, Los Alamos National Laboratory Report LA-13976-MS.

Spencer, Jr. B.F., Ruiz-Sandova, M.E. and Kurata, N. (2004), "Smart sensing technology: opportunities and challenges", *Struct. Control Health Monit.*, **11**(4), 349-368.

Wan E.A. and Van der Merwe, R. (2001), *The unscented Kalman filter*, Kalman Filtering and Neural Networks, (Ed. Haykin, S.), Wiley.

Weng, J.H., Loh, C.H. and Yang, J.N. (2009), "Experimental study of damage detection by data-driven subspace identification and finite-element model updating", *J. Struct. Eng. – ASCE*, **135**(12), 1533-1544.

Wu, Z.S., Xu, B. and Yokoyama, K. (2002), "Decentralized parametric damage detection based on neural network", *Comput. -Aided Civil Infrastruct. Eng.*, **17**(3), 175-184.

Wu, Z.S., Xu, B. and Harada, T. (2003), "Review on structural health monitoring for infrastructures", *J. Appl. Mech. - JSCE* , **6**, 1043-1054.

Xia, Y. (2011), *System Identification and Damage Detection of Nonlinear Structures*, PhD Dissertation, Department of Civil and Environmental Engineering, University of California, Irvine, CA.

Xu, B., He, J., Rovekamp, R. and Dyke, S.J. (2012), "Structural parameters and dynamic loading identification form incomplete measurements: approach and validation", *Mech. Syst. Signal Pr.*, **28**, 244-257.

Xu, B., Song, G.B. and Masri, S.F. (2012), "Damage detection for a frame structure model using vibration displacement measurement", *Struct. Health Monit.*, **11**(3), 281-292.

Yang, J.N., Huang, H.W. and LIN S.L. (2006), "Sequential non-linear least-square estimation for damage identification of structures", *Int. J. Nonlinear Mech.*, **41**, 124-140.

Yang, J.N. and Huang, H.W. (2009), "Adaptive quadratic sum-squares error for structural damage identification", *J. Eng. Mech. - ASCE*, **135**(2), 67-77.

Yang, J.N., Pan, S.W. and Huang, H.W. (2007), "An adaptive extended Kalman filter for structural damage identification II: unknown inputs", *Struct. Control Health Monit*., **14**(3), 497-521.

Yi, T.H., Li, H.N. and Gu M. (2011), "Optimal sensor placement for structural health monitoring based on multiple optimization strategies", *Struct. Des. Tall Spec.*, **20**(7), 881-900.

Yi, T.H., Li, H.N. and Sun, H.M. (2013), "Multi-stage structural damage diagnosis method based on "energy-damage" theory", *Smart Struct. Syst.*, **12**(3-4), 345-361.

Yuen, K.V., Liang, P.F. and Kuok, S.C. (2013), "Online estimation of noise parameters for Kalman filter", *Struct. Eng. Mech.*, **47**(3), 361-381.

Yun, C.B. and Min, J.Y. (2011), "Smart sensing, monitoring, and damage detection for civil infrastructures", *J. Civil Eng. - KSCE*, **15**(1), 1-14.

Yun, C.B., Lee, J.J. and Koo, K.Y. (2011), "Smart structure technologies for civil infrastructures in Korea: recent research and applications", *Struct. Infrastruct. E.*, **7**(9), 673-688.

Yun, G.J., Lee, S.G., Carletta, J. and Nagayama, T. (2011), "Decentralized damage identification using wavelet signal analysis embedded on wireless smart sensors", *Eng. Struct*., **33**(7), 2162-2172.

Zhang, H.D. and Han, Q.H. (2013), "Numerical investigation of seismic performance of large span single-layer latticed domes with semi-rigid joints", *Struct. Eng. Mech.*, **48**(1), 57-75.

Zhang, Q., Jankowski, L. and Duan Z. (2012), "Simultaneous identification of excitation time histories and parameterized structural damages", *Mech. Syst. Signal Pr.*, **33**,56-68.